Talanta 271 (2024) 125718

Contents lists available at ScienceDirect

Talanta

journal homepage: www.elsevier.com/locate/talanta

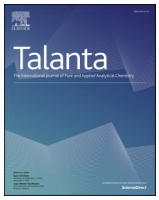

A microfluidic card-based electrochemical assay for the detection of sulfonamide resistance genes

Patrick Severin Sfragano [a,1], Eduardo Canek Reynoso [a,b,1], Norma Elena Rojas-Ruíz [c], Serena Laschi [a], Giulia Rossi [a], Martin Buchinger [a], Eduardo Torres [d,**], Ilaria Palchetti [a,*]

[a] Department of Chemistry "Ugo Schiff", University of Florence, 50019, Sesto Fiorentino, Italy
[b] Posgrado en Ciencias Ambientales, Instituto de Ciencias, Benemérita Universidad Autónoma de Puebla, Puebla, 72570, Mexico
[c] Centro de Investigaciones en Ciencias Microbiológicas, Instituto de Ciencias, Benemérita Universidad Autónoma de Puebla, Puebla, 72000, Mexico
[d] Centro de Química, Instituto de Ciencias, Benemérita Universidad Autónoma de Puebla, Puebla, 72570, Mexico

ARTICLE INFO

Handling editor: J.-M. Kauffmann

Keywords:
Antimicrobial resistance
Isothermal amplification
Recombinase polymerase amplification
Genosensor
Microfluidics
Magnetic particles

ABSTRACT

Most electroanalytical detection schemes for DNA markers require considerable time and effort from expert personnel to thoroughly follow the analysis and obtain reliable outcomes. This work aims to present an electrochemical assay performed inside a small card-based platform powered by microfluidic manipulation, requiring minimal human intervention and consumables. The assay couples a sample/signal dual amplification and DNA-modified magnetic particles for the detection of DNA amplification products. Particularly, the *sul1* and *sul4* genes involved in the resistance against sulfonamide antibiotics were analyzed. As recognized by the World Health Organization, antimicrobial resistance threatens global public health by hampering medication efficacy against infections. Consequently, analytical methods for the determination of such genes in environmental and clinical matrices are imperative. Herein, the resistance genes were extracted from *E. coli* cells and amplified using an enzyme-assisted isothermal amplification at 37 °C. The amplification products were analyzed in an easily-produced, low-cost, card-based set-up implementing a microfluidic system, demanding limited manual work and small sample volumes. The target amplicon was thus captured and isolated using versatile DNA-modified magnetic beads injected into the microchannel and exposed to the various reagents in a continuously controlled microfluidic flow. After the optimization of the efficiency of each phase of the assay, the platform achieved limits of detections of 44.2 pmol L^{-1} for *sul1* and 48.5 pmol L^{-1} for *sul4*, and was able to detect down to ≥500-fold diluted amplification products of *sul1* extracted from *E. coli* living cells in around 1 h, thus enabling numerous end-point analyses with a single amplification reaction.

1. Introduction

Year after year, the field of biosensing schemes experiences continually growing advancements, particularly in the analysis of DNA biomarkers for a variety of applications, spanning from clinical diagnostics to food safety and environmental monitoring. Numerous approaches are available nowadays to detect target DNA fragments. Many common strategies are based on sandwich-like structures that immobilize the target filament on a solid phase using a capture probe and then generate an electrochemical signal proportionate to its concentration in the sample [1]. However, such traditional methods operated in vials often involve long time-consuming and labor-intensive protocols that expert personnel have to meticulously follow through manual operations. Among the various disadvantages, which include the repetitiveness of such manual operations and the need for expert users, human error might concur with inconsistencies in the results.

In recent years, many strides have been taken in the attempt to automate and miniaturize such analytical procedures with the desire to obtain solutions easily operable by non-trained personnel, streamlining the process and reducing the potential for errors, while maintaining high sensitivities and performances. Thus, lab-on-a-chip and microfluidic systems have increasingly been developed in recent times [2]. The aim is

* Corresponding author. Department of Chemistry "Ugo Schiff", University of Florence, Via della Lastruccia 3, 50019, Sesto Fiorentino, Italy.
** Corresponding author. Centro de Química, Instituto de Ciencias, Benemérita Universidad Autónoma de Puebla, Puebla, 72570, Mexico.
E-mail addresses: eduardo.torres@correo.buap.mx (E. Torres), ilaria.palchetti@unifi.it (I. Palchetti).
[1] P. S. S. and E. C. R. contributed equally to this work.

https://doi.org/10.1016/j.talanta.2024.125718
Received 5 December 2023; Received in revised form 20 January 2024; Accepted 23 January 2024
Available online 24 January 2024

to offer more efficient approaches in DNA analysis by integrating on a compact platform all the analytical steps required for the detection. Most microfluidic platforms rely on the capture of the analyte using probes immobilized in specific areas of the device's microchannel. This is the case of the work proposed by H. Ben-Yoav and coworkers [3], in which they designed a microfluidic arrayed electrochemical lab-on-a-chip platform on polydimethylsiloxane. They used it for the label-free detection of the hybridization using oligonucleotides (30-mer) through electrochemical impedance spectroscopy. The thiolated oligos were immobilized on a gold surface through the Au-thiol interaction. A valved manipulation system was used to control the flux. They obtained a theoretical limit of detection of 1 nmol L^{-1}. Another interesting example was reported by Dincer's research group [4]. In particular, they worked on a disposable microfluidic platform for the electrochemical detection of microRNA-197 (22-mer). The immobilization of the biotinylated DNA capture probe was accomplished by coating the microchannel with streptavidin, later blocked with bovine serum albumin and biotin. After stopping the flux for a defined period (*stop-flow*), an amperometric readout was performed following a glucose oxidase-based enzymatic reaction. Such biosensor revealed a LOD of 1.27 nmol L^{-1} using 0.58 μL of sample.

Besides the direct functionalization of the microchannel, magnetic beads (MBs) provide convenient means of capturing, concentrating, and isolating target DNA fragments, while simplifying washing steps by easily separating bound and unbound molecules. This work aims to present a microfluidic-based genosensing platform to carry out the detection of DNA amplification products by using superparamagnetic microbeads [5–7]. The heart of the system is a methacrylate cartridge (microfluid card) in which a microchannel of optimized dimensions has been created. Using a suitable magnet, MBs are immobilized inside the microchannel in order to expose them to the flow of the different assay solutions [8]. In this application, the proposed MBs functionalized with a DNA capture probe are incubated with the DNA target and an enzyme-labeled signaling probe to generate an electroactive moiety upon adding an enzymatic substrate.

As a proof-of-concept, such system was optimized and tested on the detection of antimicrobial resistance genes (ARGs) found in the genome of gram-negative multi-resistant microorganisms (*e.g.*, *Escherichia coli*) [9–11]. Important examples are the *FolP* mutant genes, such as *sul1* and *sul4* [12–14]. Sulfonamides are synthetic antibiotics that act as competitive inhibitors on the enzyme dihydropteroate synthase (DHPS) belonging to the folic acid metabolic pathway, essential in synthesizing DNA and RNA in microorganisms [15,16]. Inhibiting DHPS, bacterial growth is prevented, leading to death [9,17]. The ARGs mentioned above encode a DHPS with a low affinity for sulfonamides, which becomes less effective. The *sul1* gene is of great interest since it is in the conserved region of *Int1*, a class 1 integron considered one of the leading mobile genetic elements contributing to the dissemination of Antimicrobial Resistance (AMR) [18–20]. In addition, the *sul4* gene was recently found in microorganisms in wastewater and river waters near urban areas in some Asian and European countries and presents a higher resistance potential [21]. It is thus interesting and essential to monitor the presence of such genes in environmental and clinical samples [22–24]. In this work, their detection was performed through the help of Recombinase Polymerase Amplification (RPA), an isothermal DNA amplification technique able to work at a low and constant working temperature (between 22 and 45 °C) in short times (~20 min) [25,26], without sample pretreatment and the need for specialized instruments [27–30]. By doing this, it was possible to overcome some of the limitations of common DNA amplification techniques based on polymerase chain reaction (*e.g.*, sophisticated and costly instruments, several temperature cycles, and extended analysis times) [31].

To the best of our knowledge, no other electrochemical genosensing approaches that specifically tackle the detection of *sul1* and *sul4* genes have been reported in the recent literature. As further novelties, our work deals with this detection by coupling an isothermal DNA amplification to a semi-automatable microfluidic system in view of portable methods that require reduced human intervention.

2. Materials and Methods

2.1. Materials and apparatus

D-biotin, diethanolamine, α-naphthyl phosphate, streptavidin–alkaline phosphatase from *S. avidinii* (AlkP), the non-ionic surfactant polyoxyethylene-20-sorbitan monolaurate (Tween 20), disodium hydrogen phosphate, ethylenediaminetetraacetic acid (EDTA), magnesium chloride, potassium chloride, sodium chloride, acetic acid, and Tris-HCl were purchased from Merck (Milan, Italy). Dynabeads™ MyOne™ Streptavidin C1 (streptavidin-modified magnetic beads, MBs), GeneRuler 50 and 100 bp DNA Ladders, NoLimits 250 bp DNA Fragment, Superblock™ (PBS) Blocking Buffer (cat. No. 37515), and DNase/RNase-free distilled water were acquired from ThermoFisher Scientific (Italy). Agarose RA™ and ethanol 70 % v/v were obtained from VWR (Italy). Luria broth (Miller's LB broth) was purchased from Condalab (Mexico), *N*-Lauroylsarcosine sodium (sarkosyl), Phenol:Chloroform: Isoamyl Alcohol 25:24:1 was obtained from Golden Bell (Mexico), ethanol absolute and chloroform were acquired from J.T. Baker (Mexico) and sodium acetate was purchased from Karal (Mexico).

All used oligonucleotides were designed from in-house sources based on the target sequence genes of the GenBank database (https://www.ncbi.nlm.nih.gov/genbank/) of *sul1* (NG_048081.1), *sul4* (NG_056174.1), and two non-specific genes (NM_001983.4 and NM_000123.4). The oligonucleotides were analyzed to determine the specificity using the Standard Nucleotide BLAST program (https://blast.ncbi.nlm.nih.gov/Blast.cgi). The RPA primers (forward and reverse) were obtained from Integrated DNA Technologies (www.idtdna.com) (USA), and synthetic oligonucleotides (CP, T, and SP) were purchased from Eurofins Genomics (https://eurofinsgenomics.eu/) (Italy).

sul1 gene.

Forward primer: 5′-GCCGATGAGATCAGACGTATTG-3′

Reverse primer: 5′-CTCGAAGAACCGCACAATCT-3′

Capture probe (CP): 5′-Biotin-TEG-GCCGATGAGATCAGACGTATTG-3′

Synthetic Target (T): 5′-CAGGGCGTCTAAGAGCGGCGCAATACGTCTGATCTCATCGGC-3′

Signaling probe (SP): 5′-CGCCGCTCTTAGACGCCCTG-TEG-Biotin-3′

sul4 gene.

Forward primer: 5′-CCACACTAACCAGCTTCAAATG-3′

Reverse primer: 5′-AGTTCTTCCTCTGCGCTTATAG-3′

Capture probe (CP): 5′-Biotin-TEG-CCACACTAACCAGCTTCAAATG-3′

Synthetic Target (T): 5′-TGATGTAGGTGCGTTCACCCCATTTGAAGCTGGTTAGTGTGG-3′

Signaling probe (SP): 5′-GGGTGAACGCACCTACATCA-TEG-Biotin-3′

Non-specific gene 1.

Synthetic Target: 5′-TGTGCAGTCGGCCAGGATACACATCTTAGCCAGCTCCTTGAG-3′

Non-specific gene 2.

Synthetic Target: 5′-GTGCTAATCTAAAGAAGGAATCAATTCGGAGCTGTGTCTG-3′

Such oligonucleotide sequences were purchased as pellets, subsequently reconstituted, and stored at −25 °C in Tris-EDTA buffer. All dilutions were instead prepared daily using phosphate-buffered saline (PBS). All aqueous solutions were prepared using water from a Milli-Q Water Purification System (Millipore, UK) with a resistivity of ≤18.2 MΩ cm and filtered through a sterile polyethersulfone membrane with a pore size of 0.2 μm (Sarstedt AG & Co., Italy).

Composition of the buffer solutions: **Lysis buffer**, pH 8.0: 100 mmol L^{-1} EDTA, 100 mmol L^{-1} NaCl, 50 mmol L^{-1} Tris-HCl; **Acetate buffer**, pH 7: 30 mmol L^{-1} sodium acetate; **Tris-EDTA**, pH 7.4: 10 mmol L^{-1} Tris-HCl, 1 mmol L^{-1} EDTA; **TAE-1x**, pH 8.5: 40 mmol L^{-1} Tris, 20

mmol L^{-1} CH_3COOH, and 1 mmol L^{-1} EDTA·$2H_2O$; **PBS**, pH 7.4: 136 mmol L^{-1} NaCl, 2.68 mmol L^{-1} KCl, 3.97 mmol L^{-1} Na_2HPO_4·12 H_2O, 1.46 mmol L^{-1} KH_2PO_4; **PBS-T**, pH 7.4: 0.136 mol L^{-1} NaCl, 2.68 mmol L^{-1} KCl, 3.97 mmol L^{-1} Na_2HPO_4·12 H_2O, 1.46 mmol L^{-1} KH_2PO_4, 0.01 % v/v Tween 20; **DEA**, pH 9.6: 100 mmol L^{-1} diethanolamine, 0.1 mol L^{-1} KCl, 1 mmol L^{-1} $MgCl_2$; **DEA-T**, pH 9.6: 0.1 mol L^{-1} diethanolamine, 0.1 mol L^{-1} KCl, 1 mmol L^{-1} $MgCl_2$, 0.01 % v/v Tween 20; **2×W&B** (washing and binding buffer), pH 7.2: 10 mmol L^{-1} Tris HCl, 1 mmol L^{-1} EDTA, 2 mol L^{-1} NaCl; **2×W&B-T**, pH 7.2: 10 mmol L^{-1} Tris HCl, 1 mmol L^{-1} EDTA, 2 mol L^{-1} NaCl, 0.01 % v/v Tween 20; **1×W&B**, pH 7.2: 5 mmol L^{-1} Tris HCl, 0.5 mmol L^{-1} EDTA, 1 mol L^{-1} NaCl; **1×W&B-T**: 5 mmol L^{-1} Tris HCl, 0.5 mmol L^{-1} EDTA, 1 mol L^{-1} NaCl, 0.01 % v/v Tween 20.

The electrophoresis cell was purchased from C.B.S. Scientific (MGU-202T, Italy). The screen-printed electrodes (SPEs) were obtained from Ecobioservices and Researches SrL (Sesto Fiorentino, Italy). Each SPE consisted of a carbon working electrode (⌀ 3 mm), a carbon counter electrode, and a silver pseudo-reference electrode. The electrodes were used as disposable and without any previous cleaning treatment or modification. Differential pulse voltammetry (DPV) measurements were performed using a Palmsens4 portable potentiostat or the smartphone-assisted Sensit Smart, both controlled by PSTrace 5.9 (Palmsens, Netherlands), choosing the following parameters after optimizations: potential window from −0.1 to +0.3 V, pulse amplitude of 94 mV, pulse width of 62 ms, step of 6.8 mV. All potentials herein indicated are referred to the screen-printed silver pseudo-reference electrode.

The neodymium-based magnets (NdFeB alloy) N52 used to immobilize the magnetic beads onto the surface of the working electrode and inside the microfluidic platform were purchased from Webcraft GmbH (Gottmadingen, Germany). The magnets employed are cylindrical in shape, with a diameter of 8 mm and a height of 6 mm. The microfluidic flow was established by using a compact low-pulse Minipuls® 3 peristaltic pump (Gilson, Italy), enabling liquid circulation inside the card and the PVC tubes connected (Elkay, 116-0549-030, volume: 50 μL m^{-1}, length: 455 mm, inner diameter: 0.25 mm) through positive displacement (head speed: from 0.01 to 48 rpm). Heating and temperature-controlled continuous mixings were performed using the Biosan TS-100 ThermoShaker (Bioclass, Pistoia, Italy).

2.2. Magnetic beads functionalization with the DNA capture probe

Magnetic beads (MBs) were functionalized using a biotinylated

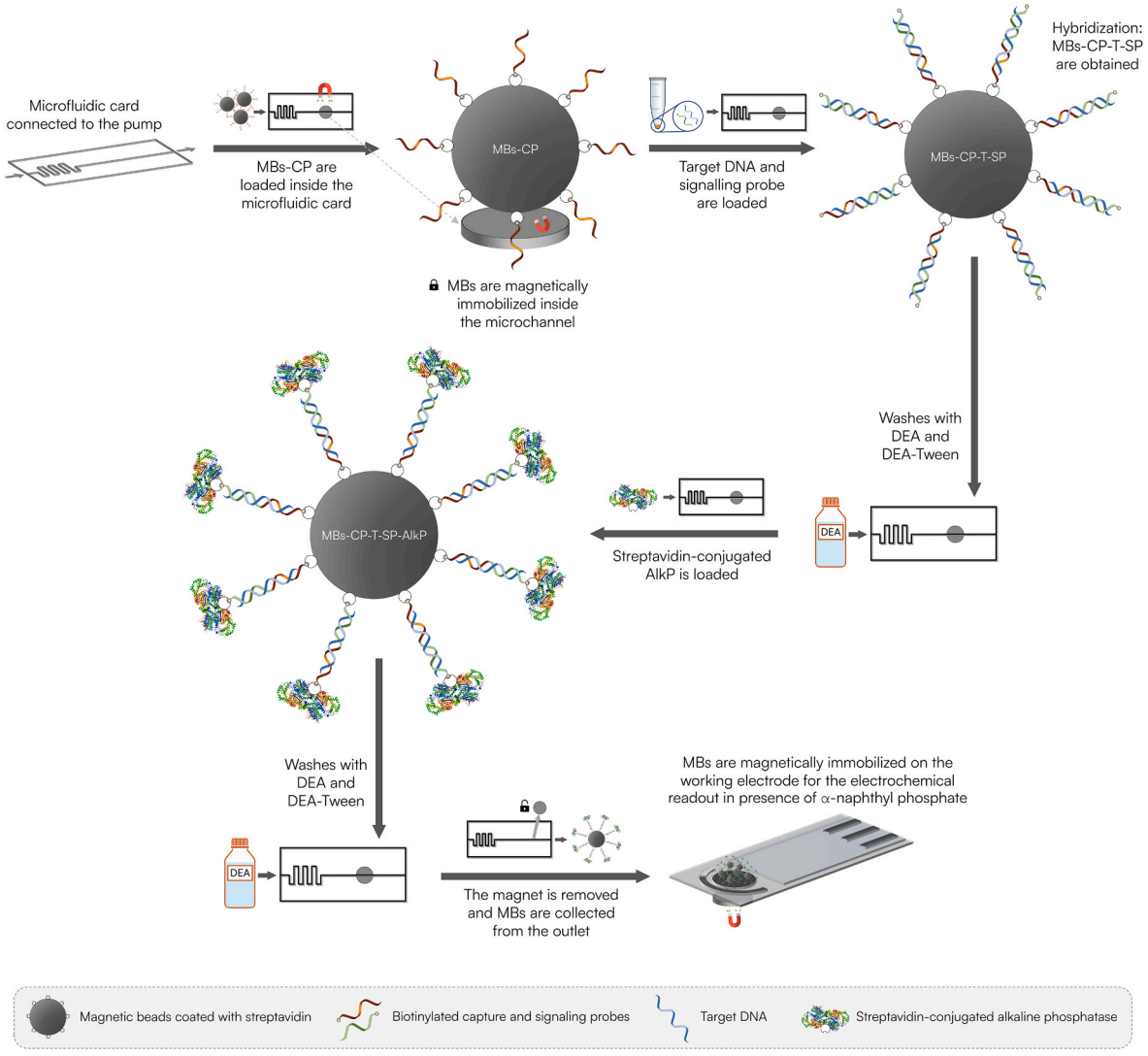

Fig. 1. Scheme of the genomagneto assay. Magnetic beads functionalized with capture probes (MBs-CP) are magnetically immobilized inside the microfluidic card. Next, target (T) and signaling probe (SP) are loaded using a peristaltic pump. After washing with DEA and DEA-T buffers, streptavidin-conjugated alkaline phosphatase (AlkP) is introduced. Once washed again with DEA and DEA-T buffers, the magnet is removed and the beads are placed on the screen-printed electrode for the electrochemical readout in the presence of α-naphthyl phosphate.

capture probe on 50-μL-aliquots of a 10 mg mL^{-1} suspension homogeneously vortexed for >30 s. The MBs were washed twice with 200 μL 2×W&B buffer and then incubated with 200 μL 1×W&B buffer containing 1 μmol L^{-1} capture probe for 30 min in an orbital rotation mixer. After washing twice with 1×W&B and once with 1×W&B-T, the obtained functionalized magnetic beads (MBs-CP) were incubated with 200 μL 1 mmol L^{-1} biotin solution in 1×W&B for 30 min under mixing to block the remaining streptavidin sites. MBs-CP were washed twice with 1×W&B-T, resuspended in 250 μL 1×W&B-T, and stored at +4 °C [32]. A magnetic particle concentrator (DynaMag™-2 magnetic rack, ThermoFisher Scientific, Italy) was used to isolate the MBs from the supernatant during the washing steps.

2.3. Scheme of the genomagneto-assay

The scheme of the proposed genomagneto-assay is described in Fig. 1. Briefly, after the functionalization of the beads, the assay is carried out using an aliquot of 10 μL of MBs-CP. These are introduced in the flow line using the peristaltic pump. At the same time, the magnets are placed in position to capture the beads by fixing them in the linear part of the card. After a first washing step, performed by flushing PBS buffer inside the microchannel, a solution containing target DNA (T, either synthetic sequences or amplified products) and signaling probe (SP) is introduced and kept in contact with the immobilized beads. After washing with DEA buffer, the hybrid MB-CP-T-SP is labeled by injecting the enzyme conjugate (AlkP) followed by another washing step with DEA(-T) buffer [33]. Finally, after the completion of the affinity reaction, the magnet is removed, and the functionalized beads (MB-CP-T-SP-AlkP) are directed through the outlet and collected in a fixed volume of DEA(-T) buffer to be incubated with the enzyme substrate (α-naphthyl phosphate) for the electrochemical measurement. Below, the complete procedure is reported, including the flow rates applied for the various steps:

1) First, the magnets are placed in position on the card.
2) 10 μL of the CP-functionalized beads resuspended in 100 μL PBS are introduced into the card's microchannel at a flow rate of 33 μL min^{-1}. The MBs-CP are thus blocked in the channel by the magnets.
3) 100 μL of a 50/50 (v/v) solution containing 190 nmol L^{-1} SP and either the target DNA (synthetic T or amplicons), the negative sample, or PBS (blank sample) were fluxed in the channel (33 μL min^{-1}). Before hybridization, in the case of amplification products, the T-SP solution is heated at 99 °C for 5 min to denature the double-stranded structure. The flow rate is slowed down to 8 (synthetic T) or 4 (amplicons) μL min^{-1}, respectively.
4) After the affinity reaction, a washing step with DEA-T buffer for 6 min at 17 μL min^{-1}, followed by the same procedure with DEA buffer.
5) A 1.5 U mL^{-1} streptavidin-AlkP solution in DEA is introduced at 33 μL min^{-1} until reaching the beads, and then incubated by decelerating the flow to 8 (synthetic T) or 4 (amplicons) μL min^{-1} for 12 or 24 min, respectively.
6) DEA-T and DEA, in sequence, are quickly injected (33 μL min^{-1}) through the system to remove unbound material.
7) The magnets are disconnected: the magnetic field ceases and the beads are released.
8) A high-speed DEA buffer flow is initiated (1 min at 360 μL min^{-1}) to direct the beads through the outlet, where they are collected in a vial and resuspended in 50 μL DEA for the electrochemical readout.

2.4. Electrochemical readout

The electrochemical readout was conducted as previously reported [8]. Briefly, 10 μL of the CP-SP-T-AlkP-modified beads, previously re-suspended in 50 μL DEA, were first deposited onto the working electrode's surface. A magnet placed underneath the electrode ensured the beads' position. Next, 60 μL of a 0.5 mg mL^{-1} solution of α-naphthyl phosphate were added to ensure coverage of all three electrodes. Following a 3-min incubation period, the electroactive α-naphthol generated by the enzymatic reaction was monitored by registering the anodic peak current intensity through differential pulse voltammetry.

2.5. Microfluidic card

Microfluidic cards were produced in-house by laser cutting from poly (methyl methacrylate) sheets with a thickness of 3 mm. The inlet-connected channel featured a serpentine segment that directs fluids along curved trajectories, followed by a straight channel leading to the outlet. The purpose of the serpentine-shaped section is to increase the channel length and passively enhance sample mixing by inducing transversal flows and chaotic advection from the interaction between channel geometry and fluids [34]. The overall channel length is 142.5 mm. The dimensions of the microfluidic card are indicated in Fig. 2a, whereas a picture of the card is displayed in Fig. 2b. At the mid-length of the linear section (approximately 23 mm far from the serpentine segment), two magnets are strategically positioned above and below the microfluidic card. The strong magnetic attraction between them ensures their stable position in the designated section, without the need for special sockets, notches, or grooves on the plastic support of the microfluidic card. This facilitates insertion and subsequent removal of the magnets during the bead release phase, since no interlocking features or constraints must be overcome.

After laser cutting, each card was cleaned with 70 % ethanol and Milli-Q H_2O, dried, and sealed with a transparent biaxially-oriented polypropylene (BOPP) film (Avery Dennison Corporation, Cadorago (CO), Italy). The BOPP film was replaced after each assay.

Inlet and outlet sides were connected to the fluidics by using commercially available needles (Terumo Neolus® Lueger 25 g x 5/8" - 0.5 × 16) attached with ethyl 2-cyanoacrylate adhesive (Loctite®, Henkel Ltd, Italy).

By using a multichannel peristaltic pump, it is possible to achieve parallelization and utilization of multiple microfluidic cards simultaneously. Each card can be connected to one of the inlets of the pump, thus processing simultaneously more samples of the same target DNA sequence (*e.g.*, distinct collected samples or/at varying concentrations), or – upon changing the capture probe immobilized on the MBs – of different sequences.

2.6. Non-specific-binding effect

In an attempt to reduce non-specific binding due to the various reagents flowing into the channels, the card's channel was coated with non-relevant proteins. Such physical surface modification exploits blocker proteins that adsorb to surfaces, such as bovine serum albumin (BSA), casein, or others. The inherent assumption of this approach is that, by coating the system with these surface-active proteins, partial inhibition of the immobilization of other molecules is provided [35]. For this purpose, two different blocking agents were tested:

- **BSA.** The microfluidic channel was filled with a 1 mg mL^{-1} BSA aqueous solution and incubated in the dark for 16 h at +4 °C. When unused, the albumin-coated card was stored at +4 °C filled with PBS.
- **Commercially available blocking buffer.** 300 μL of Superblock™ (PBS) blocking buffer (ThermoFisher Scientific, Italy) were introduced in the channel at 33 μL min^{-1} for a total time of 9 min ca. Then, Milli-Q water was rapidly flushed into the system for 1 min (360 μL min^{-1}). This process was repeated for a total of three times, alternating the injection of 300 μL blocking buffer to a washing step with water.

After each treatment, the card was used to perform a fluidic test.

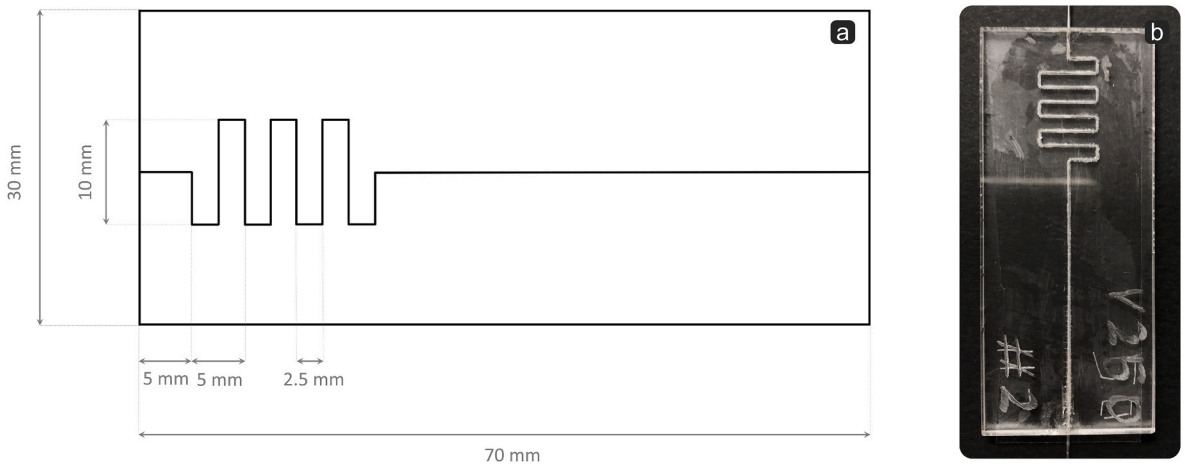

Fig. 2. **(a)** Dimensioned drawing and **(b)** picture of the microfluidic card.

2.7. Data representation and fitting

The anodic peak current (i_p) of the enzymatically-produced α-naphthol was plotted as a function of DNA concentration present in the analyzed sample. The data were fitted by nonlinear regression to the four-parameter logistic (4-PL) regression curve. The value of 0 on the logarithmic x-axis was deliberately inserted using the built-in parameters of OriginPro 2023 (OriginLab Corporation) to better highlight the presence of the blank sample. The limit of detection (LOD) was evaluated considering the average signal of the blank plus three times the standard deviation, whereas the limit of quantification (LOQ) was estimated taking into account the average response of the blank plus ten times the standard deviation. The obtained values were converted into picomoles per liter by fitting the data to the 4-PL function.

2.8. Analysis of sul1 in E. coli cells

2.8.1. Bacterial culture and DNA extraction

E. coli cells derived from NCTC 13846 obtained from Microbiologics (https://www.microbiologics.com) containing the *sul1* resistance gene were used. The bacterial lyophilized was resuspended in 5 mL of LB medium and incubated for 24 h at 37 °C. After the incubation, the bacterial cells were centrifuged at 11,000 rpm for 5 min, the liquid was separated and 150 μL of lysis buffer solution and 100 μg of lysosome were added to the pellet, the resulting solution was incubated for 30 min at 37 °C. To this solution, 22 μL of 20 % sarkosyl and 175 μL of Phenol: Chloroform:Isoamyl Alcohol were added, mixed, and centrifuged for 5 min at 11,000 rpm. Subsequently, the aqueous phase was separated, and 175 μL of Phenol:Chloroform:Isoamyl Alcohol were added again and centrifuged for 5 min at 11,000 rpm. The aqueous phase was transferred to another tube and 175 μL of chloroform was added and centrifuged at 11,000 rpm for 5 min. Subsequently, to the aqueous phase, 150 μL of ethanol absolute plus 15 μL of 3 mol L^{-1} sodium acetate pH 7 were added and incubated at −20 °C for 10 min. After the incubation, the tubes were centrifuged at 11,000 rpm for 5 min and the supernatant was removed. To the pellet, 200 μL of 70 % ethanol were added. The supernatant was discarded, and the pellet was resuspended with 25 μL of nuclease-free water and stored at −20 °C for further analyses.

2.8.2. Primer selection, isothermal amplification, and DNA purification

The *sul1*-primers were initially designed for the end-point PCR conditions, considering melting temperature (Tm), elongation, and GC content. Unlike PCR, the recommended length of RPA primers is relatively extended, with a minimum of 30 nucleotides (but typically between 32 and 35 nucleotides). However, shorter PCR primers, commonly in the range of 18–25 nucleotides as those reported in the present work, might also work, although with the probability of reduced reaction speed and sensitivity [36]. Nevertheless, such PCR-optimized primers were successfully used to perform the enzyme-assisted isothermal amplification.

Following the manufacturer's recommended protocol, the RPA reaction was performed using the TwistAmp Basic kit (TwistDx, Cambridge, UK). Briefly, a reaction mixture containing 2.4 μL of 10 μmol L^{-1} solutions of both forward and reverse primers (final concentration: 480 nmol L^{-1} each), 13.2 μL of either sterile water (negative sample) or a 50-fold diluted total DNA solution ("target" sample), and 29.5 μL of the primer-free rehydration buffer contained in the kit, was prepared. After transferring this mixture to the enzyme pellet supplied, 2.5 μL magnesium acetate 280 mmol L^{-1} (final concentration: 14 mmol L^{-1}) were added to the lids of the vials and centrifuged to make the amplification reaction start simultaneously in all samples. The tubes were then incubated at 37 °C for 20 min under continuous mixing (900 rpm). DNA purification with the Cytiva GFX™ PCR DNA and Gel Band Purification Kit (Merck, Italy) followed. Following this protocol, the 13.2 μL of DNA utilized for the RPA reaction were obtained by diluting the genomic DNA extracted by a factor of 50 in sterile water; therefore, only 0.26 μL approximately of genomic DNA are required for the amplification. On the other hand, 50 μL of the amplified sample are yielded after the purification, enough to run multiple end-point analyses through the microfluidic system. Next, the amplification products were visualized on 2 % agarose gel, using the SYBR® Safe DNA gel stain (Invitrogen) and the 6x DNA Gel Loading Dye (ThermoFisher), applying 80 V for 2 h.

3. Results and discussion

A genomagneto-assay was developed. Briefly, this was based on CP-modified magnetic beads to capture target DNA fragments inside a microfluidic card. Inside the microchannel, the magnetically-immobilized beads are exposed to the reagents described by the analytical protocol, in a continuous flow provided by a peristaltic pump (Fig. 3). *In-flow* hybridization and labeling reactions can thus occur. In the following sections, the optimization procedures of the assay steps as well as the analytical performance of the assay are discussed.

3.1. Parameter assay optimization

Assay parameters such as reagent volumes, flow rates, and incubation times needed to be optimized [32]. Such optimization measurements were mostly run with a synthetic target DNA sequence; the final optimized procedure was then applied to the analysis of isothermally-amplified *E. coli* DNA samples.

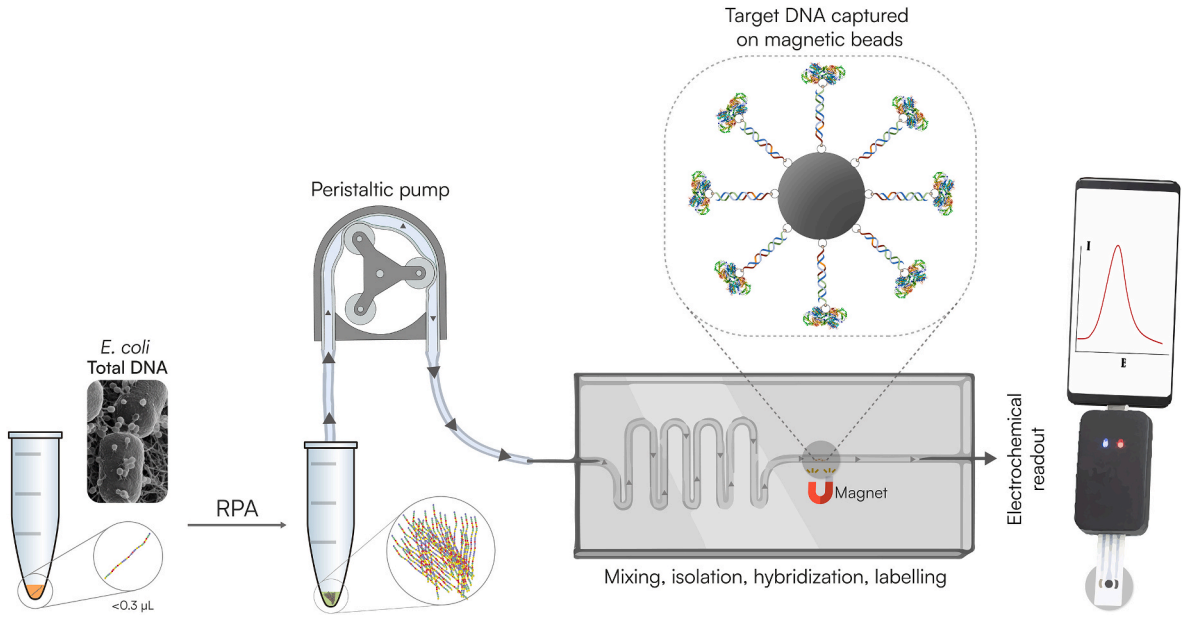

Fig. 3. Schematization of the assay design developed.

3.1.1. Optimization of flow rates, incubation times, and reagent volumes

The parameters described in previously reported magneto-assays [8, 32] were studied and optimized to work in our microfluidic setup. Experiments were thus performed to evaluate combinations of flow rates, incubation times, and reagent volumes with the aim of achieving a straightforward and efficient protocol in which every phase of the assay was optimized to improve its efficacy and efficiency, reduce reagent consumption, and decrease the overall analysis runtime. Multiple steps were conducted, as described below and, more in detail, in **Section S1** of the Supporting Information.

Step 1. Firstly, incubation times (T_{inc}) were optimized. As predictable, the most time-sensitive steps were found to be the incubation periods, especially those that characterize the exposure of the CP-functionalized beads with the T-SP complex. Initially, incubations were conducted in stop-flow, namely by pausing the microfluidic flux and waiting for the incubation times decided by protocol. However, since the results obtained in those conditions were less predictable and reproducible, with the disadvantage of drastically increasing analysis runtime, a continuously flowing approach was performed. To this end, various incubation times were tested. Unfortunately, as visible from Fig. 4a, periods below 8 min resulted in approximately halved signal-to-noise ratio (SNR) values.

Step 2. On the other hand, Fig. 4b shows that, at a constant incubation time of 8 min, improvements were instead registered by modulating the volume of T-SP flowing per unit time between 4 and 33 µL min^{-1}. With a SNR maximum at 13 µL min^{-1} in 8 min of incubation, it was possible to find the best volume of T-SP solution to be injected, which was set to 100 µL.

Step 3. Keeping a constant T-SP volume of 100 µL, additional experiments were introduced to check if the performances could further benefit by increasing the duration of the hybridization while decreasing the flow rate. To this end, we investigated four experimental conditions by which the incubation was carried out: (*i*) 6 min at 17 µL min^{-1}, (*ii*) 8 min at 13 µL min^{-1}, (*iii*) 12 min at 8 µL min^{-1}, or (*iv*) 24 min at 4 µL min^{-1}. Notably, these specific time-flow rate pairs were chosen to ensure a constant volume of T-SP injected of approximately 100 µL. With respect to the previous step, as displayed in Fig. 4c–a significant enhancement of the SNR was registered upon increasing the incubation time by 50 % in combination with a decrease of the flux speed by ~38 %.

With this in mind, the next measures were similarly dedicated to adjusting the individual flow rates of each step of the analytical protocol

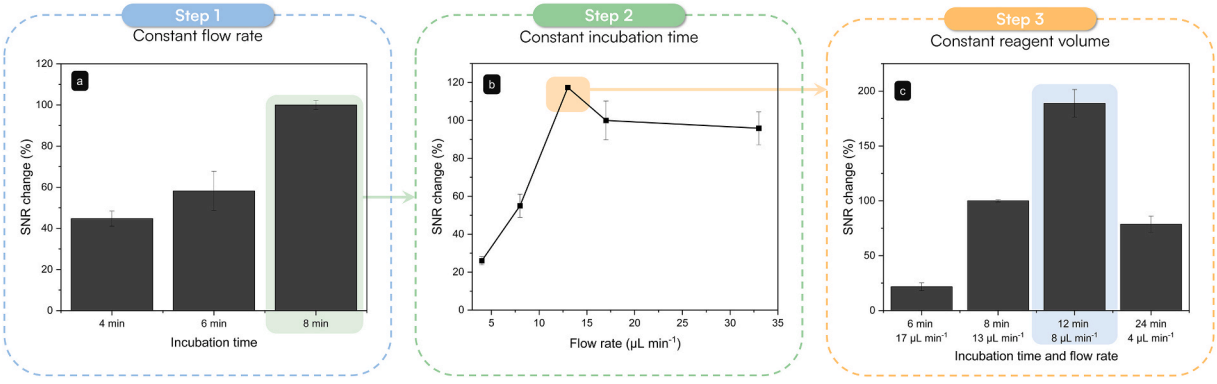

Fig. 4. Optimization plan of incubation times and flow rates with synthetic genes. **(a)** Impact of incubation times between CP-functionalized magnetic beads and the T-SP conjugate at constant flow rates. **(b)** Effect of the flow rate and consequent T-SP volumes on an 8-min hybridization. **(c)** Influence of the combination of a longer incubation with slower flow rates using constant volumes of T-SP (~100 µL). The results are expressed as % of SNR change (considering a T sample of 10 nmol L^{-1} T) from the previous optimization step introduced to better highlight the efficacy of all alterations to the protocol.

to reduce reagent consumption, decrease analysis time, improve the efficacy of all washes, and optimize the efficiency of each phase. Table S1 (SI) reports the parameters before and after optimization. The general idea was to modulate the duration of the various phases based on their time sensitivity. Thus, incubation times were prolonged by slowing the head speed of the peristaltic pump, whereas loading and washing stages were performed at higher speeds, although considering that a larger flux rate could displace magnetically less-retained beads. Practically, the protocol with constant flow rates was found to last 92 min approximately. Remarkably, the final optimized workflow decreased this latter time by >40 %, requiring less than 1 h (54 min).

3.1.2. Fouling effect

As reported in Fig. 5a–a gradual increase in the signal intensity, especially in the blank sample, was noticed after performing multiple analyses with the same card. This was identified as a sort of "memory effect" due to the previous use of the card. To better understand this behavior, a series of experiments were conducted. In particular, starting with a freshly prepared card, three subsequent cycles of analysis were performed at constant flow rates using a blank sample (0 nmol L^{-1} T), followed by T samples at concentrations of 0.1, 1, and 10 nmol L^{-1} respectively. As it can be experimentally observed, by increasing the number of experiments performed on the same card, a dramatic blank signal increase could be observed, reaching values almost 10-fold higher than on the first use (Fig. 5a). As a result, the signal-to-noise ratio (SNR), namely the ratio between the signal for a T sample and the corresponding blank was drastically reduced. This could be explained by leftover hybridized beads, free AlkP, or unbound SP-AlkP conjugates from previous measurements. Indeed, upon disassembling the card used in these experiments, an important accumulation of brown magnetic particles was noticed inside the card's cavity and on the cover tape (Fig. 5b), suggesting possible contaminations. To address this issue, attempts by priming the microchannel with BSA or commercial blocking buffer were conducted, as discussed in detail in **Section S2** of Supporting Information. Unfortunately, these solutions resulted in being unideal. A more practical solution was found in substituting the pressure-sensitive heat-activated adhesive tape on the card after every cycle of experiments. This allowed for discarding the most contaminated part of the platform and performing deep cleaning procedures of the card's cavity and the microfluidic channel with 70 % ethanol and water, thus eliminating all beads leftovers and sources of contamination. This characteristic grants the possibility of reusing almost indefinitely the microfluidic card, while discarding only the least expensive and the most recyclable module of the whole system. Changing the cover tape led to sufficiently low blank signals, that could be roughly considered as the sole product of auto-hydrolysis of the phosphate group from α-naphthyl phosphate due to environmental conditions (*e.g.*, light, heat, etc.) in the final steps.

3.2. Test on synthetic sul1 and sul4 genes

Following the optimized protocol, the developed microfluidic platform was finally applied in an assay development. Firstly, this was tested on synthetic *sul1* and *sul4* genes. Calibration curves were obtained by plotting the anodic peak current (i_p) of α-naphthol produced enzymatically as a function of DNA concentration in the range 0–10 nmol L^{-1} (Fig. 6a and b). Particularly, the y-axis displays the Δi_p, namely the difference between the signal registered at a specific T concentration and the corresponding current measured in the blank sample (0 nmol L^{-1} T). With this setup, a LOD of 44.2 pmol L^{-1} and a LOQ of 129.7 pmol L^{-1} were obtained for the *sul1* synthetic gene, whereas the *sul4* synthetic sequence exhibited a LOD of 48.5 pmol L^{-1} and a LOQ of 233.6 pmol L^{-1}.

Samples containing the *sul1*, *sul4*, and two non-specific genes, together with a blank solution (without target DNA), were also analyzed to evaluate the biosensor's specificity. In particular, using MBs functionalized with a CP specific only against the *sul1* sequence, all genes were processed with the microfluidic genomagneto-assay described at a concentration of 10 nmol L^{-1}, except the *sul1* gene, which had a concentration of 1 nmol L^{-1}. None of the genes tested exhibited a significant response, compared to that obtained with the target *sul1* gene (Fig. 6c). Hence, the detection protocol meets the specificity characteristics thanks to the high affinity of nucleic acids that strongly bind only to their complementary nucleotide sequences.

3.3. Applicability to real sample analysis: amplified sul1 gene detection

To evaluate the applicability of the developed microfluidic genomagneto-assay with real samples, it was tested on the detection of the *sul1* gene in genomic DNA extracted from cells of *Escherichia coli*. In particular, 0.26 μL of genomic DNA (31.2 ng) obtained from the culture were subjected to isothermal amplification and purified according to the protocol described in the 'Materials and Methods' section. Detailed results of the gel electrophoresis are reported in **Section S3** and Fig. S1 of the Supporting Information, considering the specificity of the reaction with two negative samples.

The obtained *sul1* amplicons were diluted with dilution factors of 10, 25, 50, 100, 250, and 500. Each sample was then analyzed in triplicate following a slightly modified version of the microfluidic protocol described in the previous sections. Indeed, when dealing with short amplification products or small oligonucleotides, as shown before, the system was found to correctly capture the target DNA and provide good

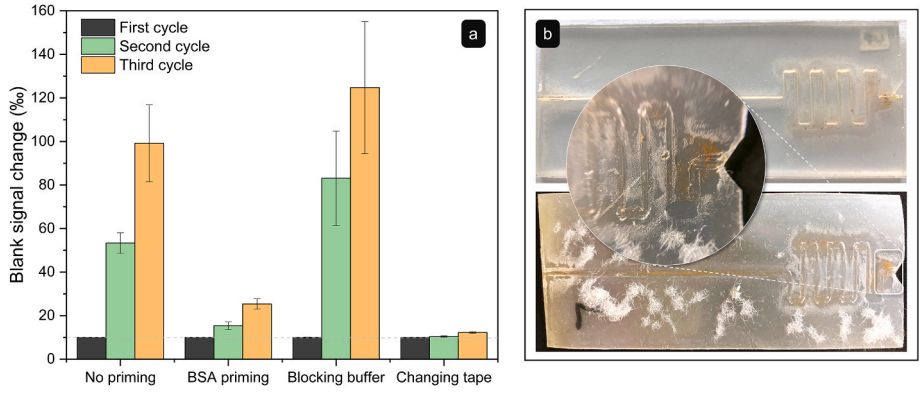

Fig. 5. (a) Signal increase with blank samples due to contaminations from previous cycles of experiments on the same platform as untreated, primed with BSA or a commercial blocking buffer, or after changing the tape before every new cycle. The results are normalized on the first use. In each cycle of experiments, target DNA samples at 0, 0.1, 1, and 10 nmol L^{-1} are analyzed through the microfluidic system. **(b)** Pictures of the microfluidic card's cavity (top) and its cover tape (bottom + inset) that show the brown microparticle leftovers after numerous experiments.

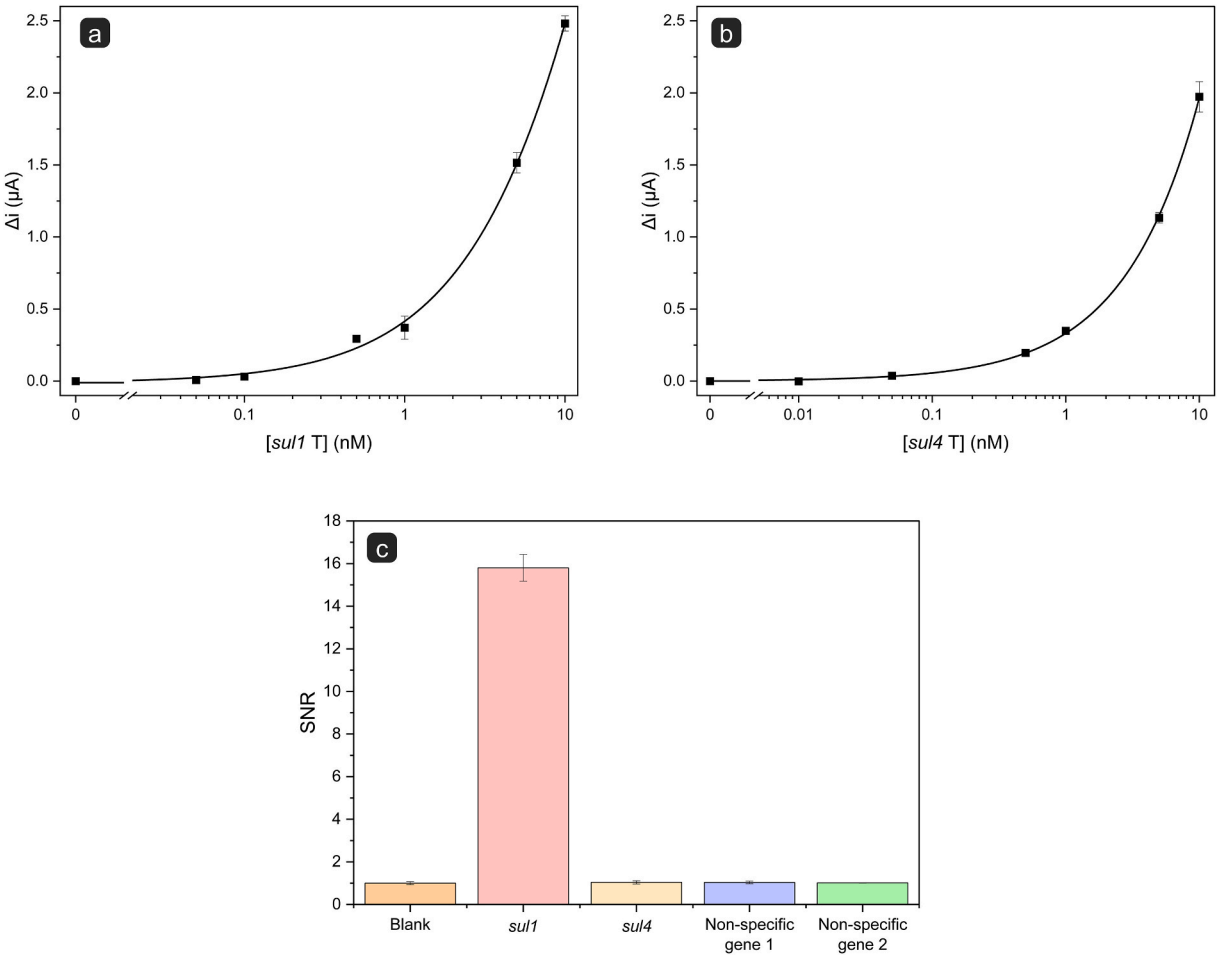

Fig. 6. Calibration functions obtained with the synthetic **(a)** *sul1* and **(b)** *sul4* sulfonamide resistance genes processed with the microfluidic protocol. The difference between the response at the various T concentrations and the corresponding blank sample is plotted as a function of T concentration. **(c)** Selectivity assay against different synthetic sequences using magnetic beads functionalized with *sul1*-complementary DNA probes.

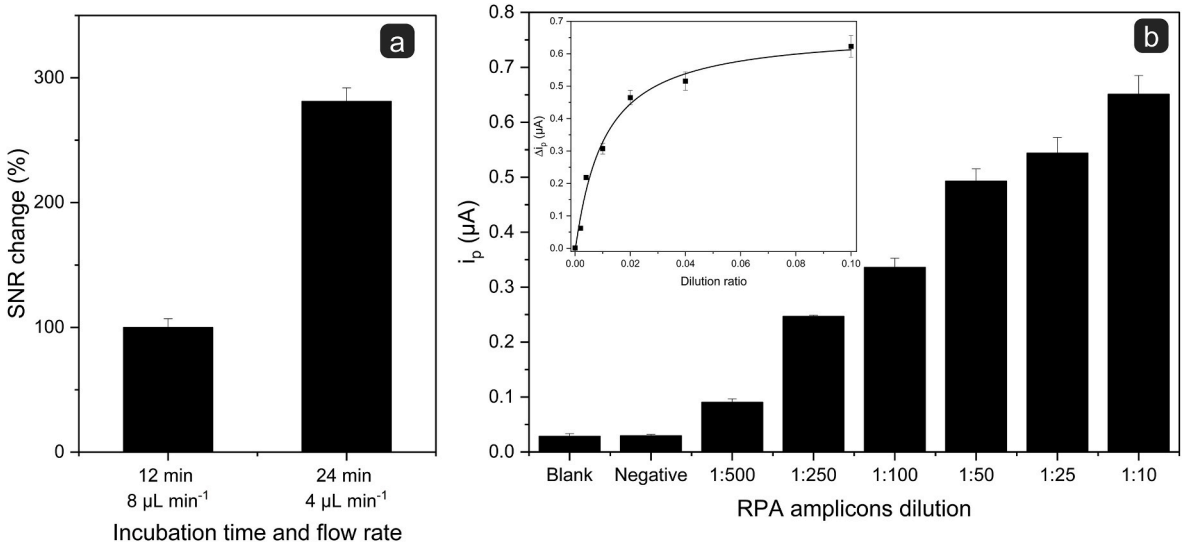

Fig. 7. Analysis of *sul1* amplicons through the microfluidic system. **(a)** Prolonged incubation times during CP-T-SP hybridization and AlkP labeling, coupled with slower flow rates, resulted in better results with long amplification products. **(b)** 10- to 500-fold diluted amplicons analyzed with the microfluidic approach, together with blank (in the absence of T) and negative (amplicon without genomic DNA) samples; the inset shows the difference between the signal obtained at the various amplicon dilutions and the corresponding blank sample as a function of the dilution ratio.

performances. On the other hand, when testing on longer amplification products, such as the *sul1* amplicon of 288 bp (which is almost 7 times larger than the synthetic T oligonucleotide), it was observed that prolonged incubation periods at slower flow rates during the crucial steps (*i.e.*, related to the CP-T-SP hybridization and the AlkP labeling) could provide better results (Fig. 7a). This is probably explainable by the fact that longer DNA sequences may require longer times to complete the hybridization and achieve better molar coverages on the beads, and slower fluxes might help this process. Thus, in the case of amplification products, the incubation time was doubled (24 min) while also halving the flow rate (4 μL min^{-1}) during the two most critical steps, namely the hybridization and the labeling. Notably, it has to be highlighted that, in doing so, the total amount of T-SP and AlkP was kept unchanged, hence the improvement was solely introduced by enhancing the interaction between the moieties.

Thus, an electrochemical readout was carried out with the various dilutions of the amplification products, together with the negative (amplicon without genomic DNA) and the blank (non-amplified sample in the absence of T) samples (Fig. 7b). To confirm what was previously observed in the agarose gel electrophoresis, the negative sample showed a negligible signal, comparable to that of the blank. A signal-to-noise ratio above 3 was instead observed for the 500-fold diluted amplicon. Moreover, plotting the difference between the response at the various amplicon dilutions and the blank as a function of the dilution factor suggested that even higher dilution factors could be introduced (inset of Fig. 7b). It can thus be concluded that, to assess the presence of the target *sul1* gene marker under these conditions, starting from a very low volume of DNA extract (0.26 μL), only 1/500 of the total volume of amplification product is required to obtain a valuable response. Indeed, obtaining amplicons with high specificity using a simple enzymatic-based amplification like RPA, able to work at low constant temperatures, represents a significant advantage in time, reagent consumption, instruments, and operability compared to PCR, which is why its use for incorporation into emerging *in situ* devices, such as biosensors, stands out [9].

4. Conclusions

In this work, a cost-effective microfluidic-based bioassay coupled to superparamagnetic microbeads for the detection of DNA amplification products was developed and applied to the detection of ARGs.

AMR is a global threat that endangers the efficacy of modern medicine against infections. To this end, the *sul1* gene, a marker for the resistance against sulfonamide antibiotics, was analyzed inside an easily produced microfluidic card and captured/isolated exploiting the versatility of DNA-functionalized magnetic beads. In a controlled microfluidic flow, the *sul1*-modified particles were exposed to the various reagents of the assay, so that hybridization and enzymatic labeling reactions could occur. The parameters linked to all phases were optimized (*i.e.*, addressing contamination sites, adjusting flow rates, monitoring incubation times in a continuously flowing flux, etc.). As a proof-of-concept, total DNA was extracted from *E. coli* cells and the *sul1* gene was selectively amplified at 37 °C through RPA. The microfluidic approach was able to detect down to ≥500-fold diluted amplification products, thus enabling numerous experiments with a single amplification reaction.

The advantages provided by the proposed platform in terms of simplicity and applicability in point-of-care conditions, and cost-effectiveness might promote its use over more complex and time-consuming solutions. Indeed, this goes in line with the tendency to miniaturize and reduce the materials required in analytical protocols (*e.g.*, disposable plastic and consumables) and with the need for simple, fast, and easy-to-operate techniques to determine antimicrobial resistance genes with applicability in clinical and environmental samples. This is considerably true in developing countries, where the shortage of trained personnel and the low funds add up to increased vulnerability to AMR for their unprivileged healthcare infrastructure and widespread misuse of antibiotics [37,38].

Finally, a full automatization of the herein-proposed approach can be envisaged by implementing software-assisted mechanisms to control the injection and release of the reagents into the microchannels. The introduction of an *in-flow* isothermal amplification conducted inside the microfluidic card will also be investigated. To this end, the possibility of using magnetic beads to provide efficient *in-flow* capture and isolation of the amplicons without the need for previous complex DNA purification methods will be evaluated.

Funding

Eduardo Canek Reynoso was funded by the "Consejo de Ciencia y Tecnología del Estado de Puebla" (CONCyTEP, Puebla, Mexico) through the grant to international research (06/2022); by "Consejo Nacional de Ciencia y Tecnología" (CONACyT) (Grant Number 754592); Financial support from the "Instituto de Ciencias" of the "Benemérita Universidad Autónoma de Puebla" for international internship. Ilaria Palchetti acknowledges the financial support from Regione Toscana Bando Salute 2018 (Research project CUP n. D78D20000870002).

CRediT authorship contribution statement

Patrick Severin Sfragano: Writing – review & editing, Writing – original draft, Investigation, Data curation. **Eduardo Canek Reynoso:** Investigation, Formal analysis. **Norma Elena Rojas-Ruíz:** Supervision. **Serena Laschi:** Writing – review & editing, Supervision. **Giulia Rossi:** Investigation. **Martin Buchinger:** Investigation. **Eduardo Torres:** Writing – review & editing, Supervision, Funding acquisition. **Ilaria Palchetti:** Writing – review & editing, Writing – original draft, Supervision, Project administration, Methodology, Funding acquisition, Conceptualization.

Declaration of competing interest

The authors declare that they have no known competing financial interests or personal relationships that could have appeared to influence the work reported in this paper.

Data availability

Data will be made available on request.

Appendix A. Supplementary data

Supplementary data to this article can be found online at https://doi.org/10.1016/j.talanta.2024.125718.

References

[1] P.S. Sfragano, S. Pillozzi, I. Palchetti, Electrochemical and PEC platforms for miRNA and other epigenetic markers of cancer diseases: recent updates, Electrochem. Commun. 124 (2021) 106929, https://doi.org/10.1016/j.elecom.2021.106929.

[2] H. Bai, Y. Wang, X. Li, J. Guo, Electrochemical nucleic acid sensors: competent pathways for mobile molecular diagnostics, Biosens. Bioelectron. 237 (2023) 115407, https://doi.org/10.1016/j.bios.2023.115407.

[3] H. Ben-Yoav, P.H. Dykstra, W.E. Bentley, R. Ghodssi, A controlled microfluidic electrochemical lab-on-a-chip for label-free diffusion-restricted DNA hybridization analysis, Biosens. Bioelectron. 64 (2015) 579–585, https://doi.org/10.1016/j.bios.2014.09.069.

[4] H. Kutluk, R. Bruch, G.A. Urban, C. Dincer, Impact of assay format on miRNA sensing: electrochemical microfluidic biosensor for miRNA-197 detection, Biosens. Bioelectron. 148 (2020) 111824, https://doi.org/10.1016/j.bios.2019.111824.

[5] F. Bettazzi, A. Romero Natale, E. Torres, I. Palchetti, Glyphosate determination by coupling an immuno-magnetic assay with electrochemical sensors, Sensors 18 (2018) 2965, https://doi.org/10.3390/s18092965.

[6] F. Bettazzi, L. Enayati, I.C. Sánchez, R. Motaghed, M. Mascini, I. Palchetti, Electrochemical bioassay for the detection of TNF-α using magnetic beads and

disposable screen-printed array of electrodes, Bioanalysis 5 (2013) 11–19, https://doi.org/10.4155/bio.12.293.
[7] A.J. Killard, L. Micheli, K. Grennan, M. Franek, V. Kolar, D. Moscone, I. Palchetti, M.R. Smyth, Amperometric separation-free immunosensor for real-time environmental monitoring, Anal. Chim. Acta 427 (2001) 173–180, https://doi.org/10.1016/S0003-2670(00)01015-1.
[8] F. Bettazzi, S. Orlandini, L. Zhang, S. Laschi, M.M. Nilsen, A. Krolicka, T. Baussant, I. Palchetti, A simple and selective electrochemical magneto-assay for sea lice eDNA detection developed with a Quality by Design approach, Sci. Total Environ. 791 (2021) 148111, https://doi.org/10.1016/j.scitotenv.2021.148111.
[9] C. Agyare, V. Etsiapa Boamah, C. Ngofi Zumbi, F. Boateng Osei, Antibiotic use in poultry production and its effects on bacterial resistance, in: Antimicrob. Resist. - A Glob. Threat, IntechOpen, 2019, https://doi.org/10.5772/intechopen.79371.
[10] N. Wang, X. Yang, S. Jiao, J. Zhang, B. Ye, S. Gao, Sulfonamide-resistant bacteria and their resistance genes in soils fertilized with manures from jiangsu province, southeastern China, PLoS One 9 (2014) e112626, https://doi.org/10.1371/journal.pone.0112626.
[11] M. Zhuang, Y. Achmon, Y. Cao, X. Liang, L. Chen, H. Wang, B.A. Siame, K.Y. Leung, Distribution of antibiotic resistance genes in the environment, Environ. Pollut. 285 (2021) 117402, https://doi.org/10.1016/j.envpol.2021.117402.
[12] F. Xu, F. Min, J. Wang, Y. Luo, S. Huang, M. Chen, R. Wu, Y. Zhang, Development and evaluation of a Luminex xTAG assay for sulfonamide resistance genes in Escherichia coli and Salmonella isolates, Mol. Cell. Probes 49 (2020) 101476, https://doi.org/10.1016/j.mcp.2019.101476.
[13] M. Sánchez-Osuna, P. Cortés, J. Barbé, I. Erill, Origin of the mobile di-hydropteroate synthase gene determining sulfonamide resistance in clinical isolates, Front. Microbiol. 9 (2019) 3332, https://doi.org/10.3389/fmicb.2018.03332.
[14] Y. Zhou, J. Fang, Z. Davood, J. Han, D. Qu, Fitness cost and compensation mechanism of sulfonamide resistance genes (sul1 , sul2 , and sul3) in Escherichia coli, Environ. Microbiol. 23 (2021) 7538–7549, https://doi.org/10.1111/1462-2920.15783.
[15] M. Wainwright, J.E. Kristiansen, On the 75th anniversary of Prontosil, Dyes Pigments 88 (2011) 231–234, https://doi.org/10.1016/j.dyepig.2010.08.012.
[16] S.B. Christensen, Drugs that changed society: history and current status of the early antibiotics: salvarsan, sulfonamides, and β-lactams, Molecules 26 (2021) 6057, https://doi.org/10.3390/molecules26196057.
[17] P. Lees, L. Pelligand, E. Giraud, P. Toutain, A history of antimicrobial drugs in animals: evolution and revolution, J. Vet. Pharmacol. Therapeut. 44 (2021) 137–171, https://doi.org/10.1111/jvp.12895.
[18] M. Nowrotek, E. Kotlarska, A. Łuczkiewicz, E. Felis, A. Sochacki, K. Miksch, The treatment of wastewater containing pharmaceuticals in microcosm constructed wetlands: the occurrence of integrons (int1–2) and associated resistance genes (sul1–3, qacEΔ1), Environ. Sci. Pollut. Res. 24 (2017) 15055–15066, https://doi.org/10.1007/s11356-017-9079-1.
[19] M.A. Toleman, T.R. Walsh, Combinatorial events of insertion sequences and ICE in Gram-negative bacteria, FEMS Microbiol. Rev. 35 (2011) 912–935, https://doi.org/10.1111/j.1574-6976.2011.00294.x.
[20] J. Wu, J. Wang, Z. Li, S. Guo, K. Li, P. Xu, Y.S. Ok, D.L. Jones, J. Zou, Antibiotics and antibiotic resistance genes in agricultural soils: a systematic analysis, Crit. Rev. Environ. Sci. Technol. 53 (2023) 847–864, https://doi.org/10.1080/10643389.2022.2094693.
[21] M. Razavi, N.P. Marathe, M.R. Gillings, C.-F. Flach, E. Kristiansson, D.G. Joakim Larsson, Discovery of the fourth mobile sulfonamide resistance gene, Microbiome 5 (2017) 160, https://doi.org/10.1186/s40168-017-0379-y.
[22] E.C. Reynoso, S. Laschi, I. Palchetti, E. Torres, Advances in antimicrobial resistance monitoring using sensors and biosensors: a review, Chemosensors 9 (2021) 232, https://doi.org/10.3390/chemosensors9080232.
[23] N.G. Jha, D.S. Dkhar, S.K. Singh, S.J. Malode, N.P. Shetti, P. Chandra, Engineered biosensors for diagnosing multidrug resistance in microbial and malignant cells, Biosensors 13 (2023) 235, https://doi.org/10.3390/bios13020235.
[24] S. Rentschler, L. Kaiser, H.-P. Deigner, Emerging options for the diagnosis of bacterial infections and the characterization of antimicrobial resistance, Int. J. Mol. Sci. 22 (2021) 456, https://doi.org/10.3390/ijms22010456.
[25] M. Tan, C. Liao, L. Liang, X. Yi, Z. Zhou, G. Wei, Recent advances in recombinase polymerase amplification: principle, advantages, disadvantages and applications, Front. Cell. Infect. Microbiol. 12 (2022) 1019071, https://doi.org/10.3389/fcimb.2022.1019071.
[26] I.M. Lobato, C.K. O'Sullivan, Recombinase polymerase amplification: basics, applications and recent advances, TrAC, Trends Anal. Chem. 98 (2018) 19–35, https://doi.org/10.1016/j.trac.2017.10.015.
[27] B.B. Oliveira, B. Veigas, P.V. Baptista, Isothermal amplification of nucleic acids: the race for the next "gold standard,", Front. Sensors. 2 (2021) https://doi.org/10.3389/fsens.2021.752600.
[28] O.I. Wilner, D. Yesodi, Y. Weizmann, Point-of-care nucleic acid tests: assays and devices, Nanoscale 15 (2023) 942–952, https://doi.org/10.1039/D2NR05385C.
[29] C. Patiti, P.S. Sfragano, S. Laschi, S. Pillozzi, A. Boddi, O. Crociani, A. Bernini, I. Palchetti, Chip-based and wearable tools for isothermal amplification and electrochemical analysis of nucleic acids, Chemosensors 10 (2022) 278, https://doi.org/10.3390/chemosensors10070278.
[30] M.A. Cobzariu, M.J. Lobo-Castañón, R. Miranda-Castro, Enzyme-assisted isothermal amplification of nucleic acids on the electrode surface, Curr. Opin. Electrochem. 40 (2023) 101322, https://doi.org/10.1016/j.coelec.2023.101322.
[31] X. Cao, C. Chen, Q. Zhu, Biosensors based on functional nucleic acids and isothermal amplification techniques, Talanta 253 (2023) 123977, https://doi.org/10.1016/j.talanta.2022.123977.
[32] F. Bettazzi, E. Hamid-Asl, C.L. Esposito, C. Quintavalle, N. Formisano, S. Laschi, S. Catuogno, M. Iaboni, G. Marrazza, M. Mascini, L. Cerchia, V. De Franciscis, G. Condorelli, I. Palchetti, Electrochemical detection of miRNA-222 by use of a magnetic bead-based bioassay, Anal. Bioanal. Chem. 405 (2013) 1025–1034, https://doi.org/10.1007/s00216-012-6476-7.
[33] I. Palchetti, S. Laschi, G. Marrazza, M. Mascini, Electrochemical imaging of localized sandwich DNA hybridization using scanning electrochemical microscopy, Anal. Chem. 79 (2007) 7206–7213, https://doi.org/10.1021/ac070474h.
[34] T. Rhoades, C.R. Kothapalli, P.S. Fodor, Mixing optimization in grooved serpentine microchannels, Micromachines 11 (2020) 61, https://doi.org/10.3390/mi11010061.
[35] J.Y. Lichtenberg, Y. Ling, S. Kim, Non-specific adsorption reduction methods in biosensing, Sensors 19 (2019) 2488, https://doi.org/10.3390/s19112488.
[36] J. Li, J. Macdonald, F. von Stetten, Review: a comprehensive summary of a decade development of the recombinase polymerase amplification, Analyst 144 (2019) 31–67, https://doi.org/10.1039/C8AN01621F.
[37] A. Talebi Bezmin Abadi, A.A. Rizvanov, T. Haertlé, N.L. Blatt, World health organization report: current crisis of antibiotic resistance, Bionanoscience 9 (2019) 778–788, https://doi.org/10.1007/s12668-019-00658-4.
[38] I. Ahmad Samreen, H.A. Malak, H.H. Abulreesh, Environmental antimicrobial resistance and its drivers: a potential threat to public health, J. Glob. Antimicrob. Resist. 27 (2021) 101–111, https://doi.org/10.1016/j.jgar.2021.08.001.